Polar Anchoring Strength of a Tilted Nematic: Confirmation of the Dual Easy Axis Model

Giovanni Carbone and Charles Rosenblatt

Department of Physics, Case Western Reserve University, Cleveland, Ohio 44106-7079, USA

(Received 20 October 2004; published 7 February 2005)

The polar anchoring strength coefficient W and polar pretilt angle θ_0 were measured simultaneously for the liquid crystal pentylcyanobiphenyl at a rubbed polyimide alignment layer that is ordinarily used for vertical alignment. It was found that $W \propto \theta_0^2$ over the range $0° \leq \theta_0 \lesssim 35°$. The results provide a confirmation of the dual easy axis model, wherein the liquid crystal director adopts an equilibrium orientation θ_0 at the substrate that is determined by competition between a pair of preferred orientation directions.

DOI: 10.1103/PhysRevLett.94.057802 PACS numbers: 61.30.Gd

The interactions between liquid crystal (LC) molecules and a solid substrate are of both fundamental and applied interest: Orientational transitions and wetting behavior long have occupied a prominent place in the physics of soft materials, and nearly all liquid crystal-based technologies rely on control of interfacial behavior [1]. The vast majority of scientific investigations and devices involves a nematic director ($\hat{n}$) that is oriented either perpendicular to the substrate—this is referred to as "homeotropic" or "vertical" alignment—or approximately parallel to the substrate, called "planar" alignment. Until recently it had been difficult to achieve, in equilibrium, a large polar angle θ_0 of the director at the substrate, where we define the vertical direction as $\theta_0 \equiv 0°$. Recently, however, methods have been developed that permit the so-called "pretilt angle" θ_0 to be controlled continuously up to many tens of degrees from the surface normal, facilitating the discovery of new scientific phenomena [2] and potential device development. Scharf *et al.* [3] devised a method in which a homeotropic alignment agent (silane) is printed in a grating pattern onto a planar aligning substrate (SiO_x), facilitating the full range $0° \leq \theta_0 \leq 90°$ of pretilt. Zhang *et al.* [4] used alternating vertical and horizontal corrugations to achieve a pretilt $50° \leq \theta_0 \leq 90°$. Yet another technique involves rubbing a polyimide that has a relatively rigid backbone but is designed for vertical alignment [5–7]. Our group determined [7] that a controllable and robust pretilt angle as large as 50° can be achieved using the polyamic acid SE-1211 (Nissan Chemical Industries, Ltd.) and the liquid crystal pentylcyanobiphenyl (5CB). This raises a fundamental question: Is there a single preferred axis (a so-called "easy axis") for orientation at an angle θ_0, or does $\hat{n}$ adopt an equilibrium orientation due to competition between multiple easy axes? Several results to date [8–13] point indirectly to the dual easy axis model, where one axis is approximately perpendicular to the substrate and the other is approximately parallel to the substrate. In this Letter we report on simultaneous measurements of the effective polar anchoring strength coefficient W and polar pretilt angle θ_0. In the Rapini-Papoular approximation [14] W acts like a spring constant and is defined as $\partial^2 F_{\mathrm{int}}/\partial \Delta\theta_0^2|_{\Delta\theta_0=0}$, where F_{int} is the interfacial energy (per unit area) and $\Delta\theta_0$ is the deviation at the substrate from the equilibrium polar angle θ_0. Our central result is that the coefficient $W \propto \theta_0^2$, vanishing as $\theta_0 \rightarrow 0$. The dependence of W on θ_0, moreover, provides a critical confirmation of the dual easy axis model for liquid crystal orientation.

Two indium-tin-oxide coated glass slides were spin coated with the polyamic acid SE-1211. One of the substrates was left unrubbed and baked according to the manufacturer's specifications to promote homeotropic alignment of the LC; the other substrate was overbaked and rubbed to produce a nonzero pretilt θ_0 [7]. Rubbing was accomplished using the sharp silicon stylus of an atomic force microscope over a square of size $100 \times 100\ \mu\mathrm{m}$, of which a circle $\sim 60\ \mu\mathrm{m}$ in diameter was probed optically; this method ensures that the LC-substrate interaction is spatially homogeneous. The rubbing was performed unidirectionally with a constant force, with the rubbed lines having a periodicity of 167 nm. Several force values between 1.2 and 4.8 μN were investigated, with a larger pretilt angle θ_0 associated with increasing force [7]. An unrubbed and a rubbed substrate were placed together, separated by a 50 μm thick Mylar spacer, and cemented to create a cell. The thickness d of each cell was measured by an interferometric technique [15] to within 0.2 μm, and then was filled with the LC pentylcyanobiphenyl (Merck). The optical retardation of the LC cell was measured using an automatically compensated Pockels cell, which is described elsewhere [8]. An ac voltage V at frequency 2020 Hz was applied to the cell, generating an electric field along the z axis, i.e., perpendicular to the substrates. V was ramped from 0 to 30 V rms at a rate of 2 $\mathrm{V\,min^{-1}}$ and the optical retardation of the LC was computer recorded; typical data are shown in Fig. 1. Note that all measurements were performed at room temperature, $T = 23\,°\mathrm{C}$.

Let us now turn to an analysis of the results. Defining the rubbed substrate as $z = 0$ and the unrubbed substrate

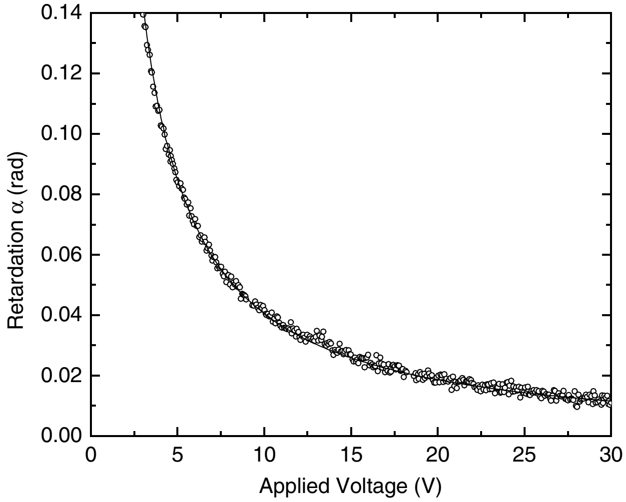

FIG. 1. Typical raw retardation data vs applied voltage (the data correspond to rubbing force 2.0 μN). Solid line represents fitted curve, with $\theta_0 = (0.194 \pm 0.002)$ rad, $W = (0.099 \pm 0.008) \times 10^{-3}\ \mathrm{J\,m^{-2}}$, and $\alpha_{\mathrm{offset}} = 0.0009$.

as $z = d$, the polar angle $\theta(z)$ of the director varies only along the z axis and is given by $\hat{n} = \hat{x}\sin\theta + \hat{z}\cos\theta$. The free energy density f can be written as $f = \frac{1}{2}K_{11}(1 + T\cos^2\theta)(d\theta/dz)^2 + D_z^2/[2\varepsilon_0\varepsilon_\perp(1 + R\cos^2\theta)] + \frac{1}{2}W\sin^2(\theta - \theta_0)\delta(z) + \frac{1}{2}W_h\sin^2\theta\,\delta(z - d)$, where $T \equiv (K_{33} - K_{11})/K_{11}$, K_{11} and K_{33} are the splay and bend elastic constants, W is the effective anchoring strength at the rubbed surface (as defined above), W_h is the anchoring strength at the unrubbed upper surface (with vertical LC alignment), $R \equiv (\varepsilon_\parallel - \varepsilon_\perp)/\varepsilon_\perp$, $\varepsilon_\perp$ and $\varepsilon_\parallel$ are the dielectric constants perpendicular and parallel to $\hat{n}$, and D_z (the z component of the electrical displacement vector, which is constant over the range $0 \le z \le d$) is given by

$$D_z = -V\varepsilon_0\varepsilon_\perp\left[\int_0^d (1 + R\cos^2\theta)^{-1}dz\right]^{-1}. \qquad (1)$$

Applying the Euler-Lagrange equation to f we obtain

$$\frac{K_{11}(1+T\cos^2\theta)}{\sin\theta\cos\theta}\frac{\partial^2\theta}{\partial z^2} = K_{11}T\left(\frac{\partial\theta}{\partial z}\right)^2 + \frac{D_z^2 R}{\varepsilon_0\varepsilon_\perp(1+R\cos^2\theta)^2}, \qquad (2)$$

or equivalently

$$\frac{1}{2}K_{11}(1 + T\cos^2\theta)\left(\frac{d\theta}{dz}\right)^2 - \frac{D_z^2}{2\varepsilon_0\varepsilon_\perp(1 + R\cos^2\theta)} = \mathrm{const.} \qquad (3)$$

The torque balance equation at the rubbed substrate is

$$K_{11}(1 + T\cos^2\theta_S)\left(\frac{d\theta}{dz}\right)_{z=0} = W\sin(\theta_S - \theta_0)\cos(\theta_S - \theta_0), \qquad (4)$$

where $\theta_S \equiv \theta\ (z = 0)$. For sufficiently large V ($V \gtrsim 2$ V) the electric coherence length ξ $[= d\{K/[\varepsilon_0(\varepsilon_\parallel - \varepsilon_\perp)]\}^{1/2}/V]$ of the nematic director is much smaller than the cell thickness d; thus, the two surfaces are decoupled, the variation of θ with z occurs only over distances of order ξ near the rubbed substrate, $\theta(z = d) \approx 0$, and $d\theta/dz_{z=d} \approx 0$. Here K is an elastic constant (more or less K_{33}), and W_h is no longer relevant to the problem for $V \gtrsim 2$ V. Additionally, note that θ_S decreases with increasing V due to an increase in the elastic torque with applied voltage. From the boundary conditions (zero pretilt and its derivative) at $z = d$ in the $V \gtrsim 2$ V limit, we can evaluate the constant in Eq. (3): $\mathrm{const} = -D_z^2/[2\varepsilon_0\varepsilon_\perp(1 + R\cos^2\theta)]$. We then find from Eqs. (3) and (4) at the $z = 0$ (rubbed) surface

$$\frac{W^2\sin^2[2(\theta_0 - \theta_S)]}{4K_{11}(1 + T\cos^2\theta_S)} - \frac{D_z^2 R\sin^2\theta_S}{\varepsilon_0\varepsilon_\perp(1 + R)(1 + R\cos^2\theta_S)} = 0. \qquad (5)$$

The numerical solution of Eq. (2), together with Eq. (1) for D_z and the boundary equation Eq. (5), provides the profile $\theta(z)$ for each set of values $\{V, W, \theta_0\}$. We approached this problem in several iterative steps to maximize computational efficiency. In the first step the profile $\theta(z)$ was assumed to be a single exponential decay of the form $\theta(z) = \tilde{\theta}_S\exp(-z/\xi)$, with $\tilde{\theta}_S \approx \theta_0 W/(W + K_{33}/\xi)$. This profile was used to evaluate the *approximate* value $\tilde{D}_z$ of the electric displacement D_z using Eq. (1). $\tilde{D}_z$ then was used to evaluate θ_S via Eq. (5), and a more accurate profile $\theta(z)$ was obtained by the numerical solution of Eq. (2). In the second iteration this new profile of $\theta(z)$ was used to obtain more accurate values for D_z and θ_S, which in turn were used to reevaluate the numerical solution $\theta(z)$ of Eq. (2). We verified that only two iterations were necessary to achieve convergence.

The profile $\theta(z)$ allows us to calculate the optical retardation α_0 through the cell for any value of the applied voltage and as a function of the two parameters W and θ_0:

$$\alpha_0 = \frac{2\pi}{\lambda}n_\perp\int_0^d\{[\cos^2\theta + (n_\parallel/n_\perp)^2\sin^2\theta]^{-1/2} - 1\}dz, \qquad (6)$$

where $\lambda = 632.8$ nm is the wavelength of the He-Ne laser beam and $n_\perp$ and $n_\parallel$ are the ordinary and extraordinary refractive indices of the LC. In principle, Eq. (6) could be used to fit the *measured* retardation α in order to obtain the two parameters W and θ_0. In practice, however, the measured retardation may not vanish as $V \to \infty$, as would be expected theoretically. For example, there could be small misalignments or strain birefringence in the glass. This requires us to introduce an additive constant α_{offset}, i.e., an offset, into Eq. (6). Thus the experimentally measured birefringence $\alpha(V)$ actually should be fitted to $\alpha_0(\theta_0, W, V) + \alpha_{\mathrm{offset}}$, where $\alpha_0(\theta_0, W, V)$ is the theoretical value in Eq. (6). Unfortunately W is very sensitive to

α_{offset}, which can be measured directly only in the limit $V \to \infty$ because the extrapolation length K_{33}/W tends to be much smaller than the electric coherence length ξ (except at very high voltage). Thus an accurate three parameter ($\theta_0, W, \alpha_{\text{offset}}$) fit is untenable. To circumvent this problem we note that α_{offset} can be eliminated by considering the experimental quantity $\bar{\alpha}(V) \equiv \alpha(V) - \alpha(\bar{V})$, which can be fitted to the theoretical form $\alpha_0(\theta_0, W, V) - \alpha_0(\theta_0, W, \bar{V})$. Here $\bar{V}$ is a sufficiently high voltage such that the retardation changes slowly with V. We arbitrarily chose $V = 28$ V, and determined $\alpha(\bar{V})$ by performing a quadratic fit to the experimental points over the range $\bar{V} - 1 < V < \bar{V} + 1$ V. This allowed us to fit the data using Eq. (6) with only two fitting parameters: W and θ_0. Additionally, to reduce the high frequency noise, the experimental data were filtered numerically by averaging both $\alpha(V)$ and V over five points. Fits were performed over the range $3 < V < 30$ V. We did not include points for $V < 3$ V (where ξ is large) for two reasons: First, our approximations that the pretilt angle and its derivative vanish at $z = d$ require that $\xi \ll d$. Second, small values of ξ were needed to avoid border effects due to the finite-sized (100×100 μm) rubbed regions. The fit was performed by minimizing the error function $\Delta_f \equiv \sum \log_{10}\{1 + |\bar{\alpha}(V) - [\alpha_0(\theta_0, W, V) - \alpha_0(\theta_0, W, \bar{V})]|\}$. This form for Δ_f was chosen to balance the weighting between the points acquired at low voltages, where the retardation is higher, and those acquired at higher voltages, where the retardation is low. To be certain that we obtained a global minimum for Δ_f we mapped the error function vs both θ_0 and W. We used the following physical parameters at $T = 23\,^\circ$C: $K_{11} = 6.51$ pN, $K_{33} = 9.04$ pN, $\varepsilon_\perp = 6.485$, $\varepsilon_{||} = 19.965$, $n_\perp = 1.539$, and $n_{||} = 1.722$, all from Ref. [16]. An example of a fit is shown in Fig. 1, and results for W vs θ_0 are shown in Fig. 2. Although W may appear to be unusually large for the more strongly rubbed regions, these values are consistent with our earlier measurements for weakly AFM-rubbed substrates [17], and with other values for W in the literature [18–20]. Also, notice that the error bars for W increase significantly when the anchoring coefficient is large, a consequence of the fact that extrapolation length K_{33}/W is small compared to the electric coherence length ξ, even at these higher voltages.

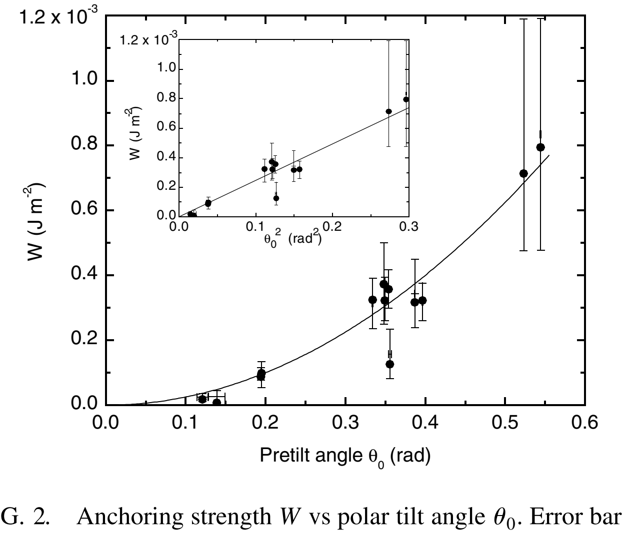

FIG. 2. Anchoring strength W vs polar tilt angle θ_0. Error bars for both the abcissa and the ordinate are shown. The solid line represents a one parameter fit to the data, $W = 2C\theta_0^2$, where $C = (1.4 \pm 0.4) \times 10^{-3}$ J m^{-2}. Inset: W vs θ_0^2.

Let us now examine the results in terms of the dual easy axis model. The total interfacial free energy at the rubbed substrate in the absence of elastic torque can be written $f_{\text{int}} = (\frac{1}{2}A\sin^2\theta_0 + \frac{1}{2}B\cos^2\theta_0 + \frac{1}{4}C\sin^4\theta_0)\delta(z)$ [8]. The coefficient A corresponds to the usual Rapini-Papoular quadratic anchoring strength coefficient for homeotropic alignment [1,14]. Rubbing of the polyimide induces alignment of the backbone, which creates a second easy axis (for planar alignment) having anchoring strength B that increases with rubbing strength [8]. Because the two easy axes (homeotropic and planar) compete, we need to introduce a higher order term in the interfacial free energy, $C\sin^4\theta_0$ with C independent of rubbing strength, to establish an equilibrium polar angle θ_0 of the director. Clearly this form for f_{int} is only approximate, as higher order terms undoubtedly are needed. Nevertheless, in the spirit of this approximation, for small θ_0 we can write $f_{\text{int}} = [\frac{1}{2}(A - B)\theta_0^2 + \frac{1}{2}B - \frac{1}{4}C\theta_0^4]\delta(z)$, which was minimized for $\theta_0 = 0$ when $B < A$ (weak rubbing) and for $\theta_0 = \sqrt{(B - A)/C}$ when $B > A$ (strong rubbing); this threshold behavior is borne out by experiment [7]. Now assume a small angular deviation $\Delta\theta_0$ from equilibrium; this would correspond to $\Delta\theta_0 \equiv \theta(z = 0) - \theta_0$. The interfacial energy becomes $f_{\text{int}} \approx [\frac{1}{2}(A - B)(\theta_0 + \Delta\theta_0)^2 + \frac{1}{2}B + \frac{1}{4}C(\theta_0 + \Delta\theta_0)^4]\delta(z)$. Keeping terms to order θ_0^2, the effective anchoring strength coefficient W, which is defined as $\partial^2 F_{\text{int}}/\partial\Delta\theta_0^2|_{\Delta\theta_0=0}$, is given by $W = B - A = 2C\theta_0^2$. Thus, for small $\theta_0 > 0$ the dual easy axis model to leading order predicts that $W \approx 2C\theta_0^2$. The polar anchoring strength is expected to increase quadratically with θ_0 (which, in turn, increases monotonically with rubbing strength), at least for sufficiently small θ_0. Of course, for weak rubbing where the director remains vertically oriented, i.e., $\theta_0 = 0$, the anchoring strength coefficient W is nonzero and is equal to $A - B$.

Figure 2 clearly demonstrates that W is nonlinear in θ_0. The inset of Fig. 2 shows W vs θ_0^2, indicating that the polar tilt angle varies approximately quadratically with θ_0, with $C = (1.4 \pm 0.4) \times 10^{-3}$ J m^{-2}. It is important to note that *if* rubbing were to result in a single, but *tilted,* easy axis there would be no reason to expect the anchoring strength to display critical behavior as $\theta_0 \to 0$. To be sure, the anchoring strength coefficient would exhibit a dependence on θ_0, but W would remain nonzero as $\theta_0 \to 0$ with weaker rubbing. But experimentally this is *not* the case. The fact that W not only vanishes as $\theta_0 \to 0$ but also that its dependence on θ_0 is quadratic is confirmation that the rubbed polyimide possesses *two* easy axes, one oriented approximately perpendicular (due to the polyimide side chains) and the other parallel (due to the polyimide backbone) to the interface. We note that there exist a few reports of both W and θ_0 for large θ_0, although these involve separate measurements [21–23] and/or measurements over large areas [24] of the two quantities, with no apparent systematic trends. We also note that temperature-dependent critical variations in W have been reported [25–29]. The vanishing of the anchoring strength *for homeotropic orientation*—this corresponds to a divergence of the tilt susceptibility—and subsequent nonzero polar tilt θ_0, all on cooling the temperature within the nematic phase, usually goes under the moniker "tilt transition." It is likely that this temperature-dependent behavior results from the presence of multiple easy axes. Returning to our experiment, although our measurements were performed only at room temperature, the fact that θ_0 for the 5CB–SE-1211 interface is highly insensitive to temperature [7] suggests that W also may be insensitive to temperature in the nematic phase. As a result, some practical benefit may accrue, since a temperature-insensitive value of W can be controlled by means of surface preparation. For example, very weak anchoring (obtained by rubbing for which B is slightly less than A) may be used to reduce significantly the threshold voltage and to alter the optical transmission characteristics of a vertically aligned liquid crystal display.

We thank Dr. Ichiro Kobayashi of Nissan Chemical Industries, Ltd., for useful conversations and a supply of SE-1211. This work was supported by the Department of Energy under Grant No. DE-FG02-01ER45934 and by the National Science Foundation under Grant No. DMR-0345109. Acknowledgment also is made to the Donors of the Petroleum Research Fund, administered by the American Chemical Society, for partial support of this research under Grant No. 37736-AC7.

[1] B. Jérôme, Rep. Prog. Phys. **54**, 391 (1991).

[2] I. M. Syed and C. Rosenblatt, Phys. Rev. E **68**, 031701 (2003).

[3] T. Scharf, S. Park, C. Padeste, H. Schift, J. Gobrecht, and J. Grupp, in Abstracts of the 20th International Liquid Crystal Conference, Ljubljana, Slovenia, 2004.

[4] B. Zhang, F. K. Lee, O. K. C. Tsui, and P. Sheng, Phys. Rev. Lett. **91**, 215501 (2003).

[5] J. C. Jung, K. H. Lee, B. S. Sohn, S. W. Lee, and M. Ree, Macromol. Symp. **164**, 227 (2001).

[6] D. Seo and S. Kobayashi, Liq. Cryst. **27**, 883 (2000).

[7] G. P. Sinha, B. Wen, and C. Rosenblatt, Appl. Phys. Lett. **79**, 2543 (2001).

[8] T. Shioda, B. Wen, and C. Rosenblatt, Phys. Rev. E **67**, 041706 (2003).

[9] I. M. Syed and C. Rosenblatt, Phys. Rev. E **67**, 041707 (2003).

[10] D. Andrienko, Y. Kurioz, Y. Reznikov, and V. Reshetnyak, Sov. Phys. JETP **85**, 1119 (1997).

[11] R. Barberi, J. J. Bonvent, M. Giocondo, and M. Iovane, J. Appl. Phys. **84**, 1321 (1998).

[12] M. Monkade, M. Boix, and G. Durand, Europhys. Lett. **5**, 697 (1988).

[13] B. Jérôme and P. Piéranski, J. Phys. (Paris) **49**, 1601 (1988).

[14] A. Rapini and M. Papoular, J. Phys. (Paris), Colloq. **30**, C4-54 (1969).

[15] C. Rosenblatt, J. Phys. (Paris) **45**, 1087 (1984).

[16] A. Bogi and S. Faetti, Liq. Cryst. **28**, 729 (2001).

[17] B. Wen and C. Rosenblatt, J. Appl. Phys. **89**, 4747 (2001).

[18] A. Sugimura, T. Miyamoto, M. Tsuji, and M. Kuze, Appl. Phys. Lett. **72**, 329 (1998).

[19] S. Stallinga, J. A. M. M. Van Heeren, and J. A. M. van den Eerenbeemd, Phys. Rev. E **53**, 1701 (1996).

[20] D.-S. Seo, K. Muroi, T. Isogami, H. Matsuda, and S. Kobayashi, Jpn. J. Appl. Phys. **31**, 2165 (1992).

[21] D.-S. Seo, S. Kobayashi, D.-Y. Kang, and H. Yokoyama, Jpn. J. Appl. Phys. **34**, 3607 (1995).

[22] D.-S. Seo and S. Kobayashi, Mol. Cryst. Liq. Cryst. **301**, 57 (1997).

[23] V. N. Raja, S. W. Kang, J. S. Lee, and J. C. Lee, Mol. Cryst. Liq. Cryst. **287**, 169 (1996); **301**, 157 (1997)

[24] Y. Toko and T. Akahane, Mol. Cryst. Liq. Cryst. **368**, 4237 (2001).

[25] G. A. DiLisi, C. Rosenblatt, A. C. Griffin, and U. Hari, Liq. Cryst. **7**, 353 (1990).

[26] P. Chiarelli, S. Faetti, and L. Franzoni, J. Phys. (Paris) **44**, 1061 (1983); Phys. Lett. **64A**, 404 (1976).

[27] K. Hiltrop and H. Stegemeyer, Ber. Bunsen-Ges. Phys. Chem. **85**, 582 (1981).

[28] H. von Känel, J. D. Litster, J. Melngailis, and H. I. Smith, Phys. Rev. A **24**, 2713 (1981).

[29] R. Barberi, M. Giocondo, M. Iovane, I. Dozov, and E. Polossat, Liq. Cryst. **25**, 23 (1998).